Cells and Materials

Volume 9 | Number 2 Article 4

1999

Quantifying the Surface Geometry of Titanium Implant Material by Different Methods of Analysis

Clara Pimienta
University of Montreal

Rashad Tawashi
University of Montreal

Cells and Materials Vol. 9, No. 2, 1999 (pages 105-115) 1051-6794/99$5.00+.25
Scanning Microscopy International, Chicago (AMF O'Hare), IL 60666 USA

QUANTIFYING THE SURFACE GEOMETRY OF TITANIUM IMPLANT MATERIAL BY DIFFERENT METHODS OF ANALYSIS

Clara Pimienta[1,*] and Rashad Tawashi[1,§]

[1]Faculty of Pharmacy, University of Montreal, Montreal, Quebec H3C 3J7, Canada; [§]Retired

(Received for publication December 24, 1996 and in revised form November 16, 1998)

Abstract

Biomaterial implant manufacturers have used rough surfaces to ensure better biocompatibility, less rejection and better adaptation of implants in the body. Proper characterization of biological interactions and biocompatibility of biomaterials requires a thorough understanding of surface complexity. Surface roughness has often been shown to be important in influencing biological reactions with the surface. Previous communications from our laboratory have described a dynamic active vision system (MVS camera) capable of measuring three-dimensional coordinates of titanium implant material surfaces. Fractal analysis, due to its straightforward relationship to texture, is used to characterize the degree of irregularity of a surface and is expressed over a range of scales with the variation method. This paper compares the fractal approach with the results of image analysis, tactile profilometry, and confocal microscopy. The data obtained in these studies show that surface fractal dimension, in particular, can be a valuable parameter to describe the complexity of surface of titanium implant materials.

Key Words: Fractal analysis, surface roughness, tactile profilometry, image analysis, confocal microscopy, biomaterials.

*Address for correspondence:
Clara Pimienta
Université de Montréal, Faculté de Pharmacie,
Case postale 6128, Succ. Centre-Ville,
Montréal (Québec)
Canada H3C 3J7

Telephone number: (514) 343-6455
FAX number: (514) 343-2102

Introduction

The goal of osseointegration of orthopedic implants is the rapid and reliable achievement of mechanically stable, long-lasting fixation between living bone and textured implant surface (Taylor and Gibbons, 1983; Meyle *et al.*, 1993). Textured surfaces can be produced by the application of plasma-spray coatings (Wang *et al.*, 1993) or through sandblasting of the surface (Gotfredsen *et al.*, 1995; Ong *et al.*, 1996). Titanium has long been a material of choice for many orthopedic and dental implant protheses because it is lightweight and durable. It can easily be prepared in many different shapes and textures without affecting its biocompatibility. The spontaneous production of an inert oxide layer on its surface upon exposure to air is believed to be responsible for the high corrosion resistance exhibited by titanium (Quinquis *et al.*, 1993).

Surface composition (Wong *et al.*, 1995), surface energy (den Braber *et al.*, 1995), surface roughness and topography (Chehroudi *et al.*, 1992; Martin *et al.*, 1995; Piattelli *et al.*, 1996; Norton, 1998) all play a role in determining the surface characteristics of implants and success or failure at the bone-biomaterial interface (Brunette, 1988; Brunette *et al.*, 1991; Schwartz and Boyan, 1994; Gray *et al.*, 1996; Esposito *et al.*, 1998). Many *in vivo* studies have demonstrated better anchorage of bone implants if they have rough surfaces (Carlsson *et al.*, 1988; Gotfredsen *et al.*, 1995: Wennerberg *et al.*, 1996b; 1998). Several authors measured the torque removal force of orthopedic screws with different surface treatments and found a general trend of increasing removal torque with increasing surface roughness (Chong-Hyun and Dong-Hoo, 1994; Wennerberg *et al.*, 1995; 1996a, b; Han *et al.*, 1998). Thomas and Cook (1985) reported that implants with a rough surface had greater interface strength and higher surface coverage by bone than smooth polished implants which tended to be encased by fibrous tissue. Wennerberg *et al.* (1996b) investigated the histologic response to rough and smooth implants in cancellous bone. Implants blasted with 75 μm Al_2O_3 particles showed statistically significant differences with respect to percentage bone-to-metal contact

Table 1. Surface fractal dimension data on titanium biomaterial surfaces obtained by laser-active 3D vision described in Pimienta *et al.* (1994). Measurements were performed in triplicate and are significantly different ($p \leq 0.05$).

	Coarse titanium (A)	Fine titanium (B)	Uncoated surface (C)
Surface fractal dimension	2.31 ± 0.0	2.20 ± 0.0	2.09 ± 0.0

compared to machined implants after 12 weeks in rabbit bone.

Quantitative description of the roughness of materials and the search for new tools to characterize surfaces are becoming more important not only to assess the effect of roughness on biological interactions (Taborelli *et al.*, 1997; Bourauel *et al.*, 1998) but also to simplify the reproduction of specimens (Ratner *et al.*, 1987) and to reduce batch to batch variations. Roughness can be visualized by scanning electron microscopy or light microscopy at different levels of resolution. However, quantifying the degree of roughness can be time-consuming and complex (Lausmaa and Kasemo, 1990).

Although surface topology can greatly influence osseointegration of an implant material, it is difficult to assess which of the various parameters for quantifying surface topology are the most appropriate. Surface roughness is often characterized by measuring the altitude of different points of the surface with respect to a reference plane by means of tactile or optical techniques (Cielo, 1988). Instruments with different resolutions and scan lengths yield different values of these statistical roughness parameters for the same surface. The underlying problem with conventional methods is that although rough surfaces contain roughness on a large number of length scales, characterization parameters depend entirely on instrument resolution or sample length. A logical solution to this problem is to use scale invariant parameters to characterize rough surfaces.

The notion of fractal dimension is very close to our intuitive definition of roughness (Pentland, 1984, 1985). Mandelbrot's (1982) original definition of a pure fractal object includes another aspect, namely, infinite scaling or self-similarity. This means that no matter at what magnification we observe such a fractal object, its texture and hence its fractal dimension remain the same. Fractal dimension is directly related to the regular notion of dimension and is not an integer but rather a fractional number (between 1 and 2 for a curve, and between 2 and 3 for a surface) correlating with the space-filling property of a curve or surface (Chesters *et al.*, 1989; Gagnepain and Roques-Carmes, 1986).

The objective of this study was to characterize the surface roughness of titanium implant materials by comparing the roughness parameters of samples by tactile profilometry, confocal microscopy and image analysis of boundary lines (used to confirm the thickness of coating) with those previously derived from three-dimensional (3D) surface analysis and using the fractal approach.

Materials and Methods

All measurements were conducted on two plasma-coated titanium plates and an uncoated control plate (APS Materials Inc., Dayton, Ohio). The titanium plates were coated by the manufacturer with titanium particles deposited on commercially pure titanium surfaces by thermal spray process. Basically, thermal spray coatings are applied by injecting materials into an electric arc flame where they are heated to a molten or semi-molten state and propelled onto the substrate at high velocities. The coating is deposited particle by particle until the desired thickness is achieved. The capability of plasma to alter surface physical and chemical properties without affecting the bulk properties of materials is advantageous in the design, development and manufacture of biocompatible biomaterials (Nicholson, 1983; Ratner *et al*, 1987). The samples were used as received from the manufacturer. The surface topology of each sample was examined by scanning electron microscopy (SEM, JEOL JSM-820, JEOL USA, Peabody, MA).

Laser-active 3D vision system

The laser-active 3D vision system allows the measurement of 3D coordinates on sample surfaces. We have described the experimental details of this method in an earlier report (Pimienta *et al.*, 1994). Briefly, two titanium plasma-coated surfaces (A and B) and an uncoated surface (C) were analyzed. Scanning electron micrographs showed that surface A had a coarser texture than surface B. Surface C constituted a reference point. Three areas (4.8 mm x 24 mm) of each surface were scanned. At each position on the sample, a value for the height of surface z (x,y) was obtained from a dedicated vision processor board attached to a MVS-5 camera (Modular Vision Systems, Montreal, Quebec, Canada).

Data were acquired by optical profilometry and processed to obtain 3D reconstruction depth profiles of the study surface (Table 1 and Figure 1). Surface fractal dimension was determined over a range of scales with the variation method (Dubuc *et al.*, 1989). The surface roughness of each imaged area was evaluated quantitatively using the instruments computer software

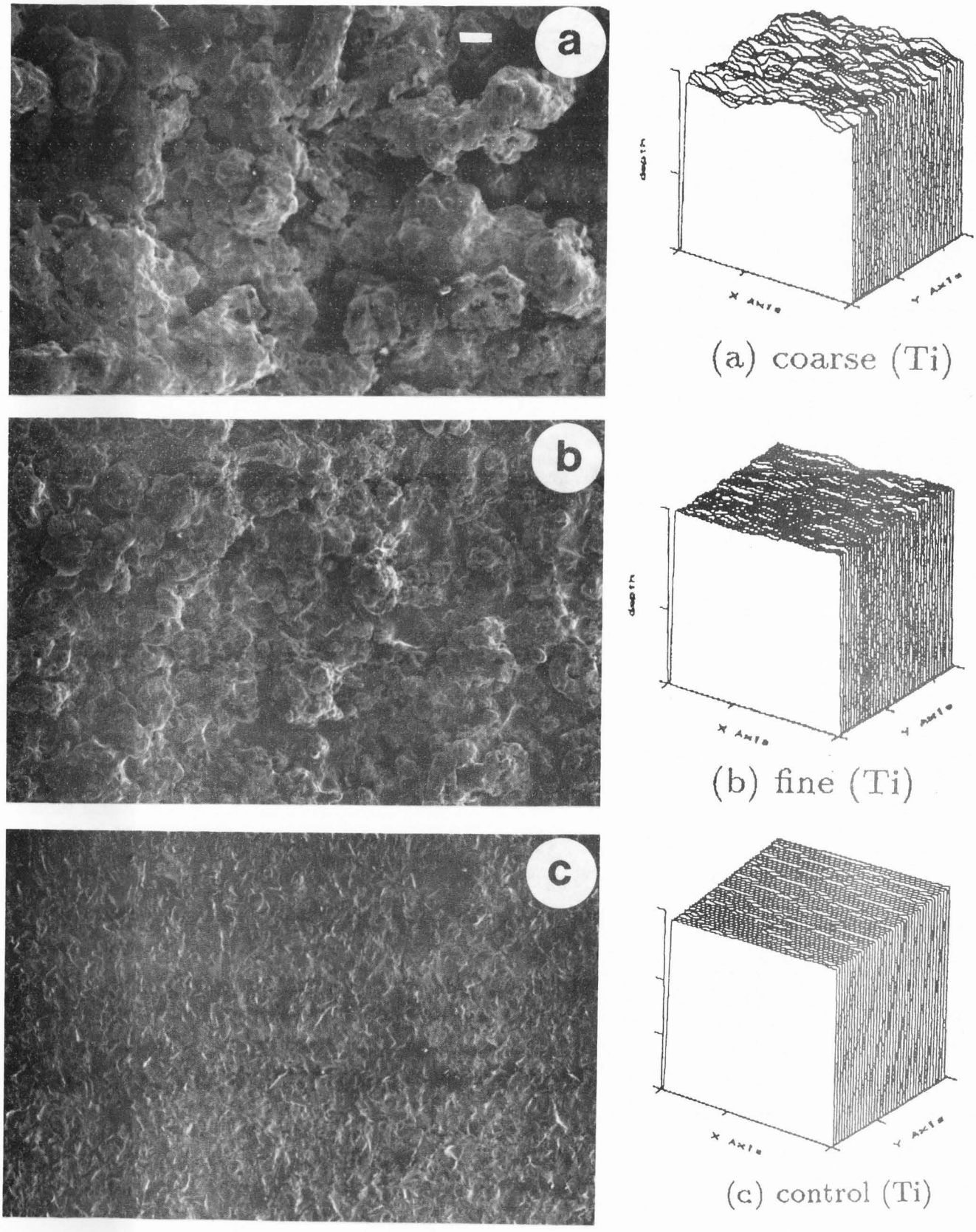

Figure 1. Scanning electron microphotographs (at left) of (a) coarse, (b) fine, and (c) uncoated titanium samples compared with their respective 3D reconstruction depth maps (at right). Bar = 100 μm.

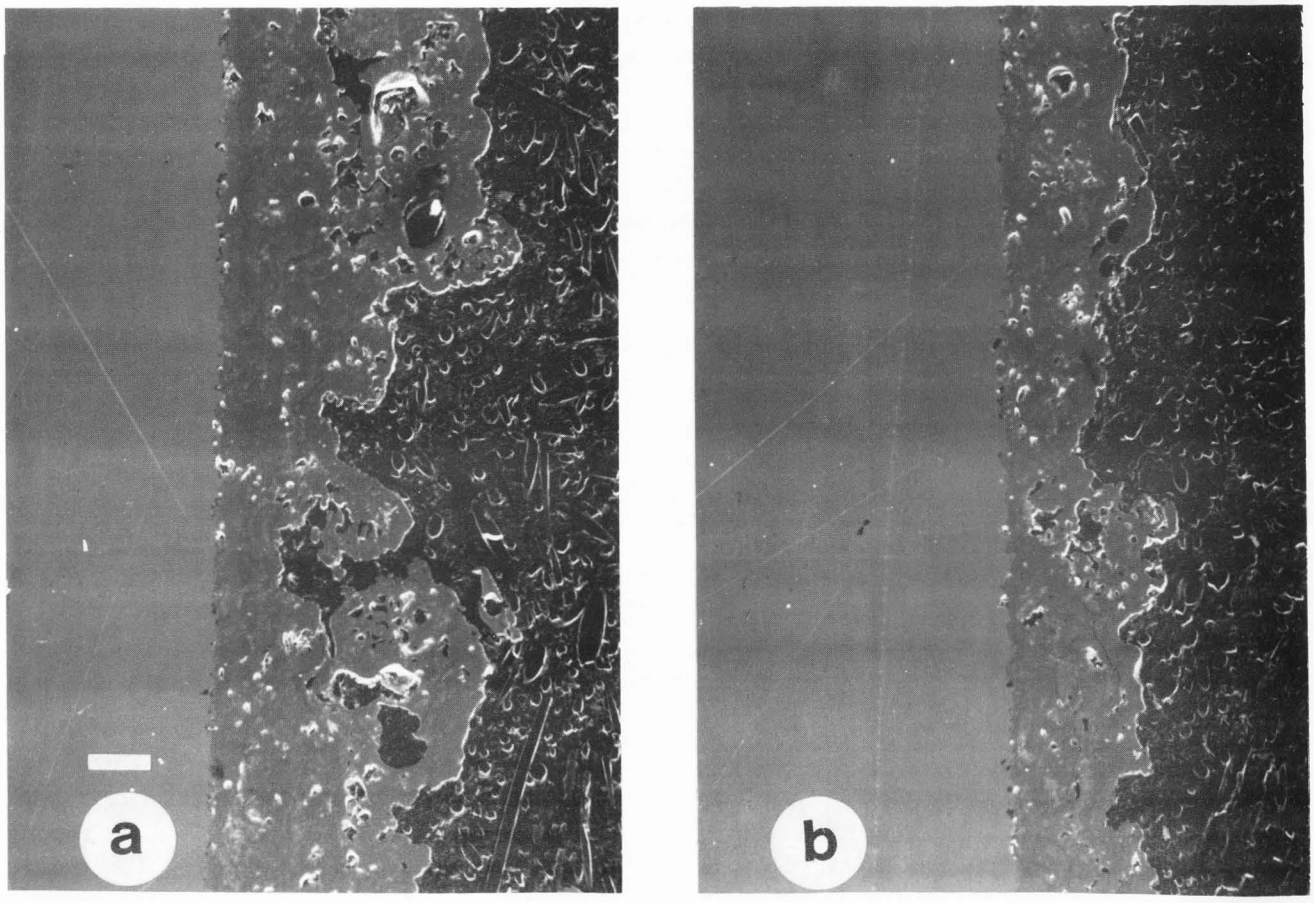

Figure 2. Scanning electron microphotographs of cross-sectional textured samples of (a) coarse and (b) fine titanium surfaces. Bar = 100 μm.

Table 2. Summary of results obtained by image analysis of boundary lines of coarse titanium and fine titanium materials. The data are expressed as means ± standard deviation (SD).

Specimen	Coating thickness (μm)	Peak height (μm)
Coarse titanium	323.35 ± 89.03	73.13 ± 65.21
Fine titanium	203.95 ± 43.0	41.03 ± 35.44

and mean values were calculated for each type of surface. Figures 1a, 1b and 1c present scanning electron micrographs of the surface and 3D plots of selected regions.

Image analysis of boundary lines

This method was used to measure the coating thickness of titanium surfaces as well as the degree of roughness. For data acquisition, samples of titanium material were diamond cut horizontally, fixed on a bakelite support and examined by SEM (JEOL JSM-820). Figure 2 presents a cross-sectional view of the material surface which simplifies analysis with the Kontron image analyzer (Kontron Bildanalyse-Image Analysis System, Munich, Germany). Figure 3 gives a brief description of the processing steps with this method. Generally, SEM images are digitized to 256 grey levels. The encoded image is smoothened, cleaned and put into contrast. Several image analysis studies (Serra, 1982) were proposed to map large voids and large particles by the erosion/dilatation method which is also applicable to surfaces. In this work, the baseline is established by the operator and does not move. A portion of the image analyzed is divided into sections and coating thickness is measured at each step (30 μm). The average of the whole image is determined and expressed as mean ± standard deviation (SD). The second variable measured is average peak height (between the highest and the lowest peak; Table 2).

Tactile profilometry

For surface roughness evaluation, stylus instruments

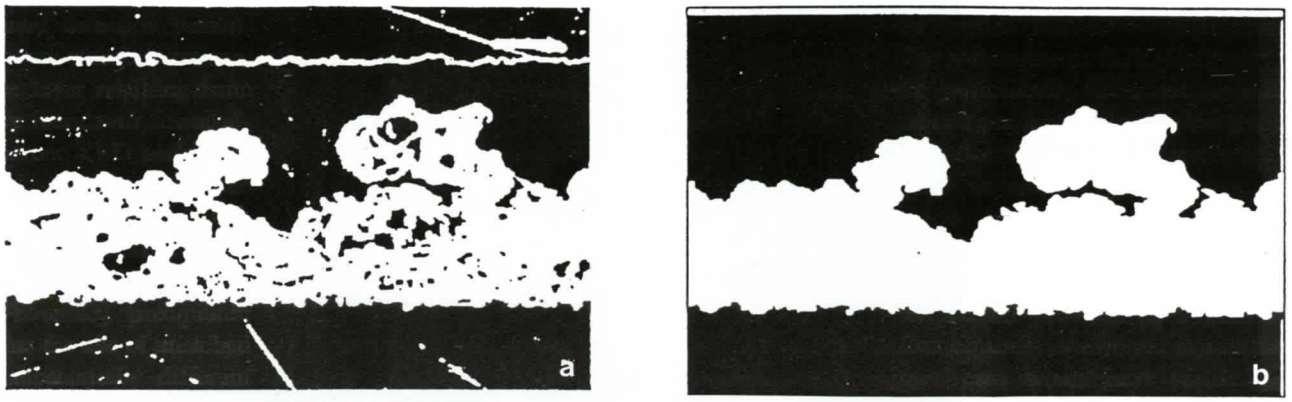

Figure 3. Image analysis method. The scanning electron microphotograph of the sample is scanned and binarized (**a**). The image is then cleaned of all small details and pores (**b**). The contact surface is put into contrast (**c**). Then, the grooves are closed (**d**) and groove depth is measured (**e**). The surface is smoothed (**f**) and peak heights are measured (**g**).

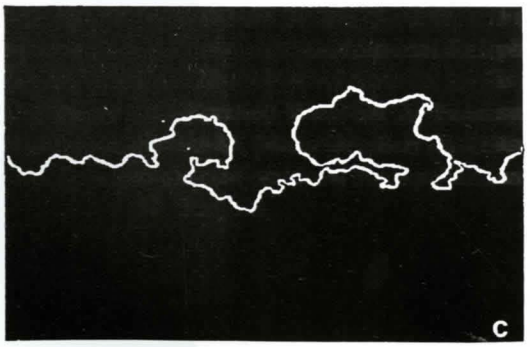

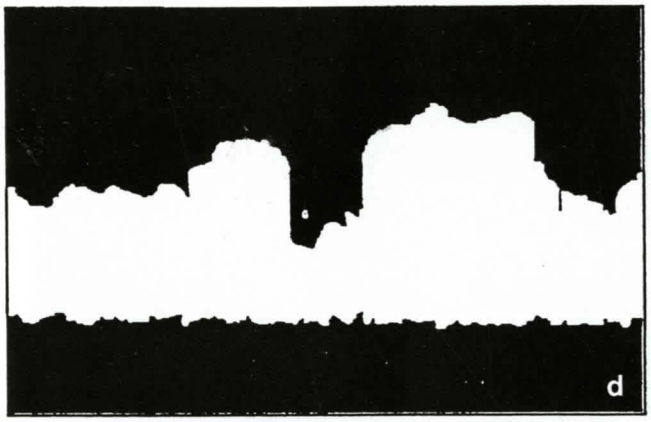

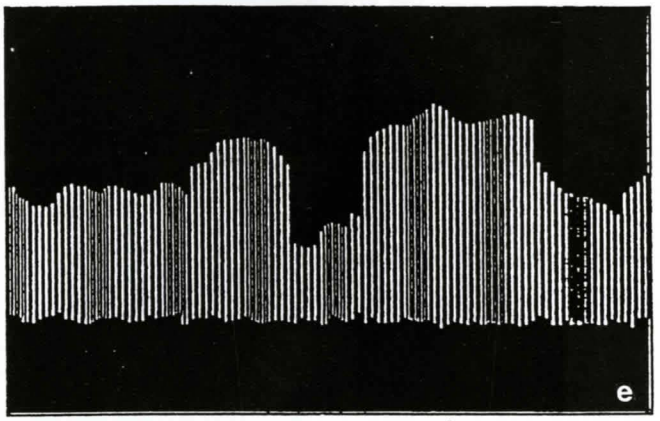

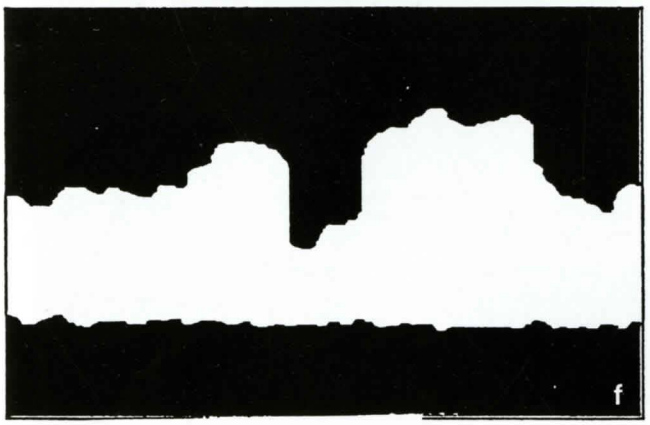

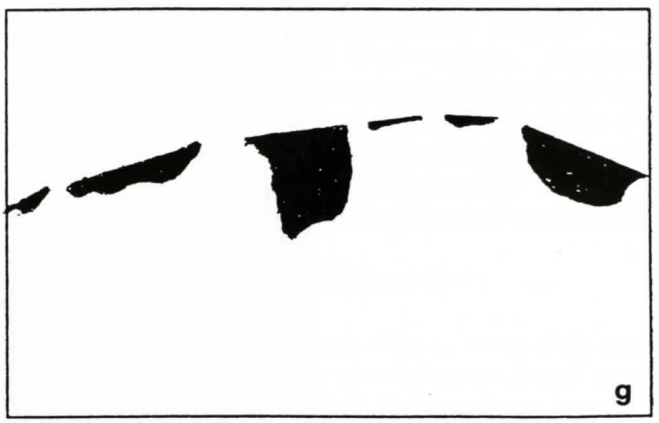

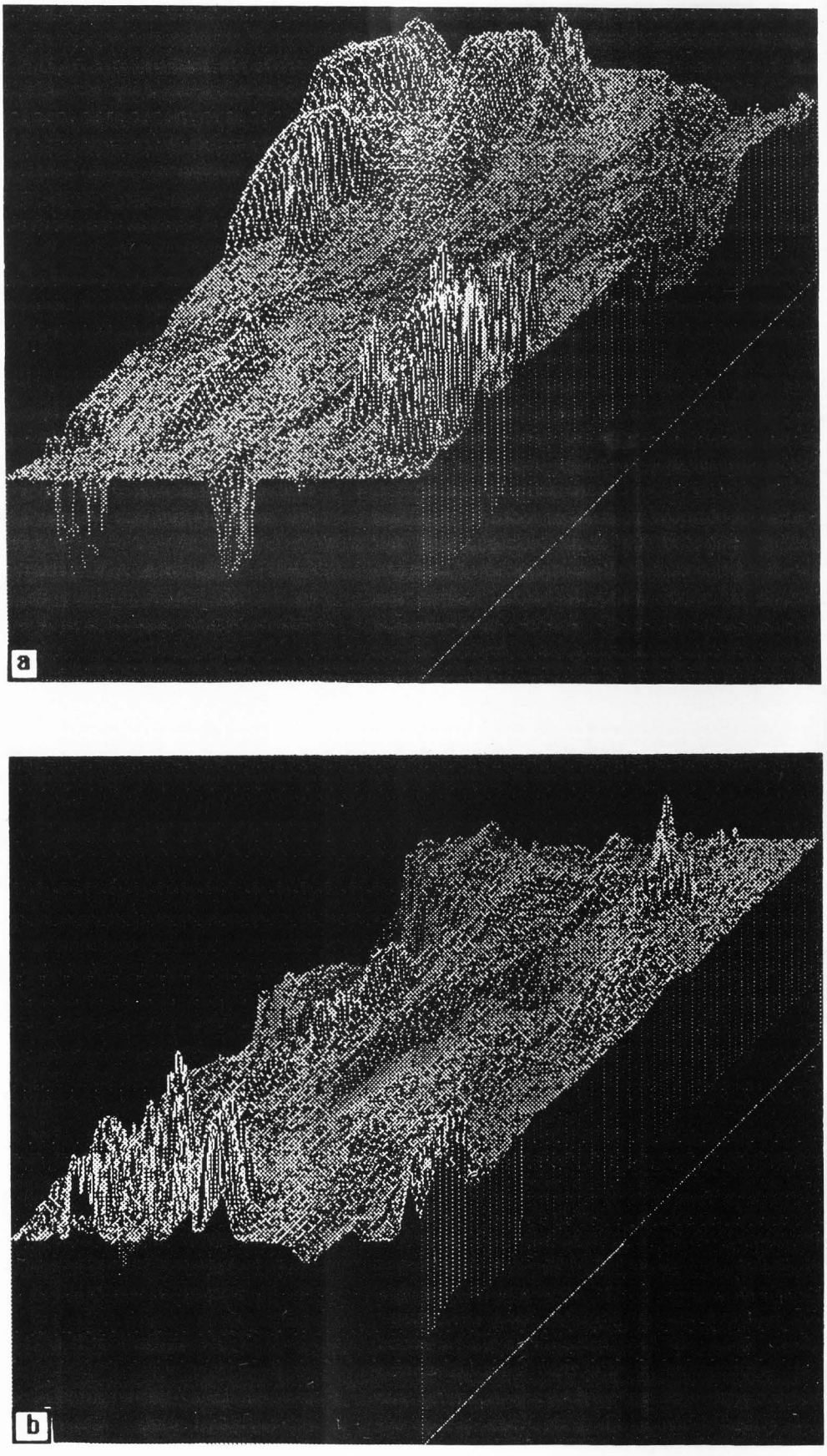

Figure 4. Three-dimensional reconstructed surfaces of (a) coarse and (b) fine titanium samples by confocal microscopy.

Table 3. Characterization of the surface roughness of different titanium implant surfaces by tactile profilometry and confocal analysis. The values obtained from uncoated surface (control) were equivalent to the standard used to calibrate the equipment.

Parameters	Tactile profilometry		Confocal microscopy	
	Coarse titanium*	Fine titanium	Coarse titanium	Fine titanium
R_a (μm)	---	26.79 ± 1.79	3.77 ± 1.03	3.64 ± 0.65
R_q(μm)	---	33.16 ± 1.54	7.23 ± 1.41	6.88 ± 0.90
R_{max}(μm)	---	175.80 ± 8.77	139.33 ± 4.71	128.40 ± 10.80
Skewness	---	---	1.41 ± 1.13	-0.99 ± 0.84

*Coarse titanium surface was outside the range of the tactile profilometer used in this study.

are standard tools for precise surface profilometry. The diamond stylus, whose tip radius typically measures some micrometers, is slowly trailed along the surface to be inspected. As it moves across the surface, the up-down motion is converted into electrical signals which are plotted against distance traversed. This method is not completely non-destructive because a small groove mark is often left along the scanned line (Cielo, 1988). However, stylus displacements represent a convolution of tip geometry and surface profile; lateral resolution is limited by stylus radius.

Tactile profilometry was conducted with a Surface Roughness Tester (Mitutoyo, Tokyo, Japan). Sampling length was 1 mm at a measuring speed of 0.5 mm/sec. The stylus is reported by the manufacturer to have a spherical tip with a radius of 5 μm on a 90° cone. Maximal horizontal range is 250 μm. The usual roughness parameters, such as the arithmetic mean of the roughness profile (R_a), the square root of the arithmetic mean (R_q) and the measured difference between the lowest and the highest points for a particular z-section (R_{max}) were calculated. Samples from the surface were analyzed 3 to 6 times. The results are expressed as means ± SD. The performance of the instrument was checked against calibrated height standards for the contact stylus.

Confocal microscopy

Confocal microscopy has the ability to discriminate against out-of-focus specimen parts by so-called optical sectioning (Kino and Corle, 1989; Carlsson and Lundahl, 1991; Ockleford, 1995). By recording a number of optical sections at various depth levels in the specimen, knowledge of the 3D structure of the specimen can be obtained. By using confocal microscopy, it is possible to improve the images lateral resolution compared to conventional microscopy.

In this study, a Leica Confocal Scanning Microscope (Leica Laser Tecknik GmbH, Heidelberg, Germany) was used. It is equipped with an argon-ion laser source (488-514 nm), fast x-y mirror scanner, high resolution z-stage (170 μm, z-movement range) and a single channel detector unit for confocal reflection or fluorescence microscopy. The pinhole setting can be made either by computer or manually but once it is set for a scan, it will not vary. The size of the pinhole was 40, the microscope objective was 16x and wavelength of the laser beam was 488 nm. The measuring range in x and y for 16x magnification was 313 X 313 μm in x,y plane and for z it was 170 μm maximum for any magnification in the x,y plane. Pixel size for 16x magnification was 0.612 μm X 0.612 μm in x,y plane. Resolution at 16x with a 0.45 numerical aperture (NA) was 2.05 μm for lateral resolution and 4.10 μm for axial resolution. Calibration followed the manufacturer's specifications prior to analysis.

Duplicate images of each surface were scanned. Images were obtained in x,y plane. The total height of the surface scanned was determined, i.e., 147 μm or 170 μm, and divided by the number of sections (i.e., 128). The height of each section was 1.15 and 1.33 μm, respectively, for each of the samples. Scanning was done line by line twice to average the intensity signal (see, Figure 4). Some pictures gave maximum information at 147 μm of depth while others were outside the limits of the instrument. Conventional roughness parameters R_a, R_q, R_{max} and skewness were determined.

Results and Discussion

The topology of the three surfaces in this study was examined by SEM (Figure 1) to obtain an overall view of surface finish and topography of the titanium samples. Surface examination (compared to uncoated surface) in

While cast dental alloys are known to undergo rapid solidification because of the large difference between the temperatures of the molten alloy and investment, Figures 1 and 2 clearly show that rapid quenching following solidification significantly affects the scale of the as-cast dendritic structure (Brantley *et al.*, 1996). This is attributed to kinetic effects associated with the much more limited time available for atomic diffusion and solute redistribution, which also resulted in the reduced density of Widmanstätten precipitates when the alloy was rapidly quenched after casting (Brantley *et al.*, 1996).

The complex interdendritic regions of these as-cast alloys contain particles of a secondary phase (Figures 4 and 5), which is assumed to account for their greater hardness compared to the palladium solid solution dendrites (Table 2). The relatively high hardness of the Pd-Cu-Ga alloy Liberty (Jelenko, Armonk, NY) has been shown to arise from the presence of a hard secondary phase, tentatively interpreted as Pd_5Ga_2 (Wu *et al.*, 1997), rather than the network of submicron face-centered tetragonal $Pd_3Ga_xCu_{1-x}$ precipitates previously proposed by Odén and Herø (1986). Transmission electron microscopic studies (Cai *et al.*, 1997) have established that the tweed structure observed by Odén and Herø (1986) in a Pd-Cu-Ga alloy with a composition similar to that of Spartan, was present in the Liberty and Spartan Plus alloys and two Pd-Ga alloys. This confirmed that the tweed structure does not account for the higher hardness of the Liberty and Spartan Plus alloys. The differences in hardness for the interdendritic regions compared to the palladium solid solution dendrites for the three Pd-Cu-Ga alloys in the present study are attributed to the presence of this hard phase (presumably Pd_5Ga_2) in the interdendritic regions. The very small size of the secondary phase particles in Figures 4 and 5 precluded accurate determinations of their composition using EDS analyses. The decrease in hardness of the alloys after heat treatments at 1500° or 1800°F (Table 1) may arise from transformation in the ultrastructure at the transmission electron microscopic level or in the microstructural transformations observed with the SEM.

Considering the composition of the three Pd-Cu-Ga alloys and the Pd-Ga phase diagram (Massalski, 1990), the equilibrium phases at 1800°F should be the palladium solid solution and the Pd_2Ga phase. As previously noted, EDS analysis suggested that the composition of the large, rounded secondary phases in the alloy specimens heat treated at 1800°F corresponded to Pd_2Ga. Moreover, Figures 9 and 10 show that the Pd_2Ga phase was found in all of the other experimental conditions investigated for these alloys and had an extreme preferred orientation in the Option alloy specimen heat treated at 1800°F. Tentative assignment of a peak near 80° to Pd_5Ga_2 for ACBC Option (Figure 9) and ACBC Spartan Plus (Figure 10) follows from the likely presence of this phase in the as-cast alloys, based upon the Pd-Ga phase diagram (Massalski, 1990), although this peak may also arise from other phases such as Pd_2Ga and the Widmanstätten precipitates. Likewise, the assignment of peaks from the specimens heat treated at 1200°F to $Pd_{13}Ga_5$ is also based upon the Pd-Ga phase diagram. Previously, the complex discontinuous precipitates found in four other high-palladium alloys after heat treatment at 1200°F were interpreted as alternating lamellae of the palladium solid solution and $Pd_{13}Ga_5$ (Wu *et al.*, 1997). Planned XRD analyses of model binary alloys having the compositions of Pd_2Ga, Pd_5Ga_2 and $Pd_{13}Ga_5$ are necessary to verify these hypotheses.

Lastly, failure to detect boron in the Option and Spartan alloys is not surprising, since both alloys contain less than 1 wt% of this element. Evidently, microsegregation during solidification to yield locally much higher boron concentrations at sites such as boundaries between dendrites and interdendritic regions, or within the interdendritic regions, does not occur. Another possibility is loss of boron during fusion of the alloy (S.P. Schaffer, private communication).

Conclusions

(1). The three Pd-Cu-Ga alloys studied (Spartan, Spartan Plus and Option) exhibited very similar microstructures and values of Vickers hardness for the different solidification and heat-treatment conditions investigated.

(2). With increasing heat-treatment temperature from 1000° to 1800°F, the Vickers hardness significantly decreased. This is attributed to the disappearance of the dendritic as-cast microstructure and transformation of the Pd_5Ga_2 hard phase, which is considered to be responsible for the high hardness and strength of the Pd-Cu-Ga alloys.

(3). The secondary phase remaining after heat treatment of the alloys at 1800°F is Pd_2Ga, while the discontinuous precipitates may consist of $Pd_{13}Ga_5$ and the palladium solid solution.

(4). Boron was not detected in Spartan and Option by the electron microprobe because of its low concentration and apparent absence of appreciable microsegregation. This small amount of boron has minimal effect on the Vickers hardness (and presumably the yield strength) of these alloys.

Acknowledgment

Support for this investigation was received from Research Grant DE10147 from the National Institute of Dental Research, Bethesda, MD 20892.

support of this work.

References

Blouet J (1988). Microgéométrie et Rugosimétrie (Microgeometry and roughness evaluation). In: Méthodes Usuelles de Caractérisation des Surfaces (Common Methods of Surface Characterization). David D, Caplan R (eds.). Eyrolles, Paris. pp. 270-289.

Bourauel C, Fries T, Drescher D, Plietsch R (1998). Surface roughness of orthodontic wires via atomic force microscopy, laser specular reflectance, and profilometry. Eur J Orthodont **20**: 79-92.

Brunette DM (1988). The Effect of surface topography on cell migration and adhesion. In: Surface Characterization of Biomaterials. Ratner BD (ed.). Elsevier Science Publishers, Amsterdam. pp. 203-217.

Brunette DM, Ratkay J, Chehroudi B (1991). Behaviour of osteoblasts on macromachined surfaces. In: The Bone-Biomaterial Interface. Davies JE (ed.). University of Toronto Press, Toronto. pp. 170-180.

Carlsson K, Lundahl P (1991). Three-dimensional specimen recording and interactive display using confocal laser microscopy and digital image processing. Mach Vis Appl **4**: 215-225.

Carlsson L, Rostlund T, Albrektsson B, Albrektsson T (1988). Removal torques for polished and rough titanium implants. Int J Oral Maxillofac Implants **3**: 21-24.

Chehroudi B, Ratkay J, Brunette DM (1992). The role of implant surface geometry on mineralization *in vivo* and *in vitro*: A transmission and scanning electron microscopic study. Cells Mater **2**: 89-104.

Chermant JL, Coster M (1987). Introduction à l'Analyse d'Images (Introduction to image analysis). J Microsc Spectrosc Electron **12**: 1-21.

Chesters S, Wen HY, Lundin M, Kasper G (1989). Fractal-based characterization of surface texture. Appl Surf Sci **40**: 185-192.

Chong-Hyun H, Dong-Hoo H (1994). A study on shear-bond strength of the interface between bone and titanium plasma-sprayed IMZ implants in rabbits. Int J Oral Maxillofac Implants **9**: 698-709.

Cielo P (1988). Surface inspection. In: Optical Techniques for Industrial Inspection. Cielo P (ed.). Academic Press, Inc., San Diego. pp. 185-257.

den Braber ET, de Ruijter JE, Smits HTJ, Ginsel LA, von Recum AF, Jansen JA (1995). Effect of parallel surface microgrooves and surface energy on cell growth. J Biomed Mater Res **29**: 511-518.

Dubuc B, Zucker SW, Tricot C, Whebi D, Quiniou JF (1989). Evaluating the fractal dimension of surfaces. Proc Roy Soc (Lon) Ser A: Math Phys Sci **425**: 113-127.

Esposito M, Hirsch JM, Lekholm U, Thomsen P (1998). Biological factors contributing to failures of osseointegrated oral implants (II). Etiopathogenesis. Eur J Oral Sci **106**: 721-764.

Feighan JE, Goldberg VM, Davy D, Parr JA, Stevenson S (1995). The influence of surface-blasting on the incorporation of titanium-alloy implants in a rabbit intramedullary model. J Bone Joint Surg **77-A**: 1380-1395.

Gagnepain JJ, Roques-Carmes C (1986). Fractal approach to two-dimensional and three-dimensional surface roughness. Wear **109**: 119-126.

Goldberg VM, Stevenson S, Feighan J, Davy D (1995). Biology of grit-blasted titanium alloy implants. Clin Orthop Relat Res **319**: 122-129.

Gotfredsen K, Wennerberg A, Johansson C, Skovgaard LT, Hjorting-Hansen E (1995). Anchorage of TiO_2-blasted, HA-coated, and machined implants: An experimental study with rabbits. J Biomed Mater Res **29**: 1223-1231.

Gray C, Boyde A, Jones SJ (1996). Topographically induced bone formation *in vitro*: Implications for bone implants and bone grafts. Bone **18**: 115-123.

Han CH, Johansson CB, Wennerberg A, Albrektsson T (1998). Quantitative and qualitative investigations of surface enlarged titanium and titanium alloy implants. Clin Oral Impl Res **9**: 1-10.

Kino GS, Corle TR (1989). Confocal scanning optical microscopy. Phys Today. **42**: 55-62.

Lausmaa GJ, Kasemo B (1990). Surface spectroscopic characterization of titanium implant materials. Appl Surf Sci **44**: 133-146.

Mandelbrot BB (1982). The Fractal Geometry of Nature. Freeman WH, (ed.). San Francisco, CA. p. 486.

Martin JY, Schwartz Z, Hummert TW, Schraub DM, Simpson J, Lankford Jr J, Dean DD, Cochran DL, Boyan BD (1995). Effect of titanium surface roughness on proliferation, differentiation, and protein synthesis of human osteoblast-like cells (MG63). J Biomed Mater Res **29**: 389-401.

Meyle J, Gültig K, Wolburg H, von Recum AF (1993). Fibroblast anchorage to microtextured surfaces. J Biomed Mater Res **27**: 1553-1557.

Nicholson DR (1983). Introduction to Plasma Theory. John Wiley & Sons, Inc., New York. pp. 1-15.

Norton MR (1998). Marginal bone levels at single tooth implants with a conical fixture design. The influence of surface macro-and microstructure. Clin Oral Impl Res **9**: 91-99.

Ockleford C (1995). The confocal laser scanning microscope (CLSM). J Pathol **176**: 1-2.

Ong JL, Prince CW, Raikar GN, Lucas LC (1996). Effect of surface topography of titanium on surface chemistry and cellular response. Implant Dent **5**: 83-88.

Pentland AP (1984). Fractal-based description of natural scenes. IEEE Trans Pattern Anal and Mach Intell **PAMI-6**: 661-674.

Pentland AP (1985). On describing complex surface shapes. Image Vis C **3**: 153-162.

Pfeifer P (1984). Fractal dimension as working tool for surface-roughness problems. Appl Surf Sci **18**: 146-164.

Piattelli A, Scarano A, Piattelli M, Calabrese L (1996). Direct bone formation on sand-blasted titanium implants: An experimental study. Biomaterials **17**: 1015-1018.

Pimienta C, Dubuc B, Tawashi R (1994). Surface fractal dimension and the quantification of roughness of titanium implant material. Cells Mater **4**: 379-386.

Quinquis P, Batifouye-Celhay C, Colat-Parros J (1993). Le Titane: Un Matériau de Choix? (Titanium: A material of choice ?). J Biom Dent **8**: 31-47.

Ratner BD, Johnston AB, Lenk TJ (1987). Biomaterial Surfaces. J Biomed Mater Res **21** (Suppl. A1): 59-90.

Schwartz Z, Boyan BD (1994). Underlying mechanisms at the bone-biomaterial interface. J Cell Biochem **56**: 340-347.

Serra J (1982). Hit or miss transformation, erosion and opening. In: Image Analysis and Mathematical Morphology. Serra J, (ed.). Academic Press, Inc. London. pp. 2-23.

Taborelli M, Jobin M, François P, Vaudraux P, Tonetti M, Szmukler-Moncler S, Simpson JP, Descouts P (1997). Influence of surface treatments developed for oral implants on the physical and biological properties of titanium. Clin Oral Impl Res **8**: 208-216.

Taylor SR, Gibbons DF (1983). Effect of surface texture on the soft tissue response to polymer implants. J Biomed Mater Res **17**: 205-227.

Thomas K, Cook S (1985). An evaluation of variables influencing implant fixation by direct bone apposition. J Biomed Mater Res **19**: 875-890.

Wang BC, Lee TM, Chang E, Yang CY (1993). The shear strength and the failure mode of plasma-sprayed hydroxyapatite coatings to bone: The effect of coating thickness. J Biomed Mater Res **27**: 1315-1327.

Wennerberg A, Albrektsson T, Andersson B, Krol JJ (1995). A histomorphometric and removal torque study of screw-shaped titanium implants with three different surface topographies. Clin Oral Impl Res **6**: 24-30.

Wennerberg A, Albrektsson T, Johansson C, Andersson B (1996a). Experimental study of turned and grit-blasted screw-shaped implants with special emphasis on effects of blasting material and surface topography. Biomaterials **17**: 15-22.

Wennerberg A, Albrektsson T, Lausmaa J (1996b). Torque and histomorphometric evaluation of c.p. titanium screws blasted with 25- and 75-μm- sized particles of Al_2O_3. J Biomed Mater Res **30**: 251-260.

Wennerberg A, Hallgren C, Johansson C, Danelli S (1998). A histomorphometric evaluation of screw-shaped implants each prepared with two surface roughnesses. Clin Oral Impl Res **9**: 11-19.

Wong M, Eulenberger J, Schenk R, Hunziker E (1995). Effect of surface topology on the osseointegration of implant materials in trabecular bone. J Biomed Mater Res **29**: 1567-1575.

Discussion with Reviewers

Reviewer I: Can the authors fully explain the fractal dimension method in sufficient details.

Authors: Fractal dimension is considered to be the space filling property closely related to complexity. It is a number between 1 and 2 for curves, and 2 and 3 for surfaces. The fractal surface model has been extended to a form which can describe complex natural 3D surfaces. One of the basic rules of the fractal concept is that the complex geometry of an object can be analyzed quantitatively if it is invariant to a transformation of scale. In other words, the same features are viewed at different magnifications. Fractal dimension, in this study, was measured by the variation method. Briefly, surface S was first dilated (Serra, 1982; Tricot *et al.*, 1988) by a horizontal square of side 2ϵ to give $S(\epsilon)$, the approximation of S at scale ϵ. Then, volume $S(\epsilon)_3$ of this dilated object was calculated. The rate of growth of $S(\epsilon)_3$ when ϵ tends to 0 is related to the fractal dimension of the object in the following way:

$$\Delta(S) = \lim_{\epsilon \to 0} \left[3 - \frac{\log |S(\epsilon)|_3}{\log \epsilon}\right]$$

where $\Delta(S)$ is the surface fractal dimension. In practice, however, Δ is obtained as the slope of a straight line fit to the log-log plot [log $(1/\epsilon)$; log $(|S(\epsilon)|_3)/\epsilon^3$]. The variation method has the property of being invariant to scale and translation (Thibert *et al.*, 1993). A detailed mathematical description of the algorithm is found in Dubuc *et al.* (1989) and the application to titanium implants has been reported by Pimienta *et al.* (1994).

Reviewer I: The results in Table 1 are based on your experiments performed in triplicate. For a physical measurement like this, would it not be relatively easy to perform more replicates and thus get greater precision? Based on the estimates of variability in Table 1, can the authors conclude that fractal dimension is better or worse than the other methods, or even, is it useful?

Authors: As shown in Table 1 the results for the different titanium surfaces and the control are significantly different and well characterized. We did not see the need to replicate the experiments, it would not have made any difference in the results. Our conclusion, based on the data obtained, indicate that the use of fractal dimension (along with the more conventional surface characterization methods) allows a better description of surface complexity. Fractal dimension can be a useful parameter in the arduous field of surface characterization and its influence on biological reactions and blood components of biomaterial implants.

Reviewer II: The number of methods compared and the number of measurements presented are both rather low, with the result that the significance of the findings is not clear.

Authors: We disagree with the reviewer, and feel that the information presented is new and of practical importance to the manufacturer of titanium implant material, particularly in quality assurance.

Reviewer V: For the Zeiss system (with which I am more familiar), it is necessary to do a z section to set parameters and calibration for the highest and lowest points in this line scan. This will determine the number of sections and therefore the thickness of the optical section that may be made.

Authors: In the Leica microscope we used, the images were acquired in x,y plane. The reviewer is correct in saying that it is necessary to set parameters for z section. Indeed, 128 sections of either 1.15 μm to 1.33 μm were scanned. However, in x,y plane, it is impossible to adjust the height of each section individually. Instead, we determined the total height of the surface we scanned, i.e., 147 or 170 μm, and divided that height by the number of sections we wished to work with, i.e., 128. Each section will be 1.15 to 1.33 μm, respectively.

Reviewer V: If the authors feel that the confocal microscope's ability to analyze a very small surface at one time is a potential pitfall, wouldn't decreasing the objective to 5x from 16x increase the sample area. Did the authors scan the samples at different magnifications to verify R_a, R_q, etc., values? Do they intrinsically change?

Authors: Changing the magnification would definitely change the size of the area and the resolution (lateral and axial). Probably with a lower magnification (the Leica has a 6.3x / 0.2 NA), we would have been able to look at a larger area and perhaps not exceed the range of the machine, i.e., 170 μm in height but resolution would have suffered. Lateral resolution with a 0.2 NA objective is 11 μm and axial resolution is 22 μm. All depends on the range of roughness we are interested in. We scanned the samples at only one magnification (16x) and the roughness at that magnification only.

Additional References

Thibert R, Dubuc B, Dufour M, Tawashi R (1993). Evaluation of the surface roughness of cystine stones using a visible diode laser scattering approach. Scanning Microsc 7: 555-561.

Tricot C, Quiniou JF, Wehbi D, Roques-Carmes C, Dubuc B (1988). Evaluation de la Dimension Fractale d'un Graphe (Evaluating the fractal dimension of a graph). Rev Phys Appl 23: 111-124.